AGU PUBLICATIONS

Geophysical Research Letters

RESEARCH LETTER
10.1002/2017GL073253

Key Points:
- The decreasing runoff efficiency trend from 1986 to 2015 in the Upper Rio Grande basin is unprecedented in the last 445 years
- Very low runoff ratios are 2.5–3 times more likely when temperatures are above-normal than when they are below-normal
- The trend arises primarily from natural variability, but runoff sensitivity to temperature implies further declines should warming continue

Supporting Information:
- Supporting Information S1

Correspondence to:
F. Lehner,
flehner@ucar.edu

Citation:
Lehner, F., E. R. Wahl, A. W. Wood, D. B. Blatchford, and D. Llewellyn (2017), Assessing recent declines in Upper Rio Grande runoff efficiency from a paleoclimate perspective, *Geophys. Res. Lett.*, *44*, 4124–4133, doi:10.1002/2017GL073253.

Received 9 DEC 2016
Accepted 2 APR 2017
Accepted article online 5 APR 2017
Published online 11 MAY 2017

Assessing recent declines in Upper Rio Grande runoff efficiency from a paleoclimate perspective

Flavio Lehner[1], Eugene R. Wahl[2], Andrew W. Wood[1], Douglas B. Blatchford[3], and Dagmar Llewellyn[4]

[1]Research Application Laboratory, National Center for Atmospheric Research, Boulder, Colorado, USA, [2]Paleoclimatology Group, NOAA's National Centers for Environmental Information, Boulder, Colorado, USA, [3]Lower Colorado Regional Office, Bureau of Reclamation, Boulder City, Nevada, USA, [4]Albuquerque Area Office, Bureau of Reclamation, Albuquerque, New Mexico, USA

Abstract Recent decades have seen strong trends in hydroclimate over the American Southwest, with major river basins such as the Rio Grande exhibiting intermittent drought and declining runoff efficiencies. The extent to which these observed trends are exceptional has implications for current water management and seasonal streamflow forecasting practices. We present a new reconstruction of runoff ratio for the Upper Rio Grande basin back to 1571 C.E., which provides evidence that the declining trend in runoff ratio from the 1980s to present day is unprecedented in context of the last 445 years. Though runoff ratio is found to vary primarily in proportion to precipitation, the reconstructions suggest a secondary influence of temperature. In years of low precipitation, very low runoff ratios are made 2.5–3 times more likely by high temperatures. This temperature sensitivity appears to have strengthened in recent decades, implying future water management vulnerability should recent warming trends in the region continue.

Plain Language Summary Since the 1980s, major river basins in the American Southwest such as the Rio Grande have experienced droughts, declining streamflow, and increasing temperatures. More importantly, runoff ratio—the portion of precipitation that ends up in the river each year, rather than evaporating—has been decreasing as well. For water managers, it is important to know whether these trends are exceptional or are merely patterns that have occurred throughout history. We use long reconstructions of historical climate based on tree rings to estimate, for the first time, the paleo runoff ratio of the Upper Rio Grande. This new record indicates that the recently observed trends in runoff ratio are unprecedented in the 445 year record. Together with precipitation, high temperatures have an important influence, making very low runoff ratios 2.5–3 times more likely. These findings suggest that runoff ratio could decrease further if warming in the region continues, which may present challenges for water management in the river basin.

1. Introduction

Streamflow in most watersheds in the American Southwest is driven primarily by winter precipitation, with a secondary contribution from summer precipitation [*Serreze et al.*, 1999]. Much of the winter precipitation falls as snow in the mountains and runs off in spring and early summer, and peak snowmelt-driven streamflows typically occur between March and July. The influence of summer precipitation increases to the south due to the increased influence of the North American monsoon [*Woodhouse et al.*, 2013], but the headwater regions of rivers such as Colorado and Rio Grande are dominated by winter precipitation. Seasonal outlooks for runoff volume driven by spring snowmelt, termed water supply forecasts (WSFs), leverage the relationship between winter precipitation and summer streamflow by using predictors such as observed winter snow water equivalent (SWE) and accumulated precipitation to forecast spring runoff. Forecasts have traditionally been made beginning in January of the same year [*Pagano et al.*, 2014]. The skill of these WSFs at longer lead times depends on both the strength and stability of the relationship between these predictors and the coming spring runoff. The runoff ratio, or the fraction of runoff generated by a given amount of precipitation, can serve as a simple metric illustrating the efficiency of this translation. Hence, decadal variations in runoff ratio would indicate nonstationarity in this translation, which in turn can alter the forecast skill. In the context of WSFs, relevant runoff ratio calculations might include the spring streamflow volume divided by winter precipitation up to the start or end of the forecast period. In the context of assessing hydroclimate variability more generally, and as necessitated by the temporal resolution of currently available paleoclimate reconstructions, total water year (October–September) streamflow and precipitation might be used.

In the American Southwest, and specifically the Upper Rio Grande basin (URG), annual runoff ratios are sensitive to a number of factors. The relative contributions of winter, spring, and summer precipitation to the water year (WY) total precipitation are important because summer precipitation typically does not contribute to streamflow as much as winter precipitation [*Hamlet et al.*, 2005], in part due to the higher evaporative losses in summer. In WSFs, for example, primarily the winter precipitation is used as a predictor, while spring and summer precipitation variability after the forecast date contributes to the forecasting uncertainty [*Pagano et al.*, 2004; *Rosenberg et al.*, 2011], especially since winter and summer precipitation in the American Southwest are not necessarily correlated on interannual time scales [*Griffin et al.*, 2013; *Coats et al.*, 2015]. Spring temperatures and wind speeds, which control evaporative loss, also influence the magnitude and timing of peak SWE in the headwaters [*Dettinger and Cayan*, 1995]. Human influences can strongly modify natural streamflows; among these, groundwater pumping [*Alley et al.*, 2002] is less easily corrected for than other impairments such as reservoir storage operations and measured diversions and return flows. Finally, recent research has suggested that dust loading on snowpack can induce earlier melt and reduced runoff volumes [*Painter et al.*, 2010].

Unexpected seasonal, interannual, or decadal variations in any of these factors can lead to WSF biases. In the URG, water resource managers have noted systematic overforecasting biases in the recent decade. The 2000s and 2010s exhibited intermittent drought conditions; thus, the forecast model's calibration over a longer period that is relatively wetter on average (i.e., including the wetter decades of the 1980s and 1990s) is likely to be a partial cause of this bias. Indeed, runoff ratios have been declining since the mid-1980s in the adjacent Upper Colorado River basin [*Woodhouse et al.*, 2016] and similar trends exist in the URG (Figure 1). Because the recent decades have also been marked by substantial upward temperature trends, the question of whether runoff ratio declines can be linked to temperature increases, and thus potentially to anthropogenic global warming, has gained the attention of the water management community [*Bureau of Reclamation*, 2016; *Udall and Overpeck*, 2017].

Assessing the long-term significance of the recent runoff efficiency changes is hindered, however, by relatively short periods of observational records for streamflow, precipitation, and SWE in many watersheds of the American West, which limit the data available for training statistical forecast models. This obstacle motivates the development of reconstructions of streamflow, precipitation, temperature, and their relationships that extend beyond the instrumental period and thus places recent variations in runoff ratio and associated forecast biases in the URG into a longer term context. There have been extensive efforts to understand hydrologic variability and improve seasonal forecasting in the Colorado River basin [*Franz et al.*, 2003], but less attention has been paid to the URG. Notably, an estimated 5 million people depend on Rio Grande water, which is shared between the U.S. and Mexico, making it one of the most allocated rivers in the world [*Dahm et al.*, 2005].

Here we use existing and new reconstructions of annual streamflow and precipitation to extend the record of runoff ratio of the URG back to 1571 of the Common Era (C.E.). We use these records to assess the extent to which observed changes in WY runoff ratio have precedent over the past 445 years. The close correspondence between WY runoff ratio and seasonal runoff ratios, as discussed above, makes this analysis relevant for water resource management. In addition, we use temperature reconstructions and a climate model simulation to investigate the role of temperature and large-scale circulation patterns in influencing periods of high and low runoff ratios.

2. Materials and Methods

2.1. Observational Data Sets

We use naturalized monthly Rio Grande streamflow at Otowi Bridge (USGS 08313000; commonly referred to as Otowi Index Supply) from 1942 to 2015 obtained from the State of New Mexico (N. Shafike, personal communication, 2016). The naturalization does not include potential impairments from groundwater pumping, the influence of which on streamflow is not currently well constrained. For precipitation and surface air temperature, we use the Parameter Elevation Regression on Independent Slopes Model data set from 1895 to 2015 [*Daly et al.*, 2008] and spatially average each field across the surface drainage area corresponding to the Otowi Bridge gauge, defined by the hydrologic unit code (HUC6) regions 130100 and 130201. For precipitation, we multiply the average value with the drainage area of this mask to convert it to units of volume.

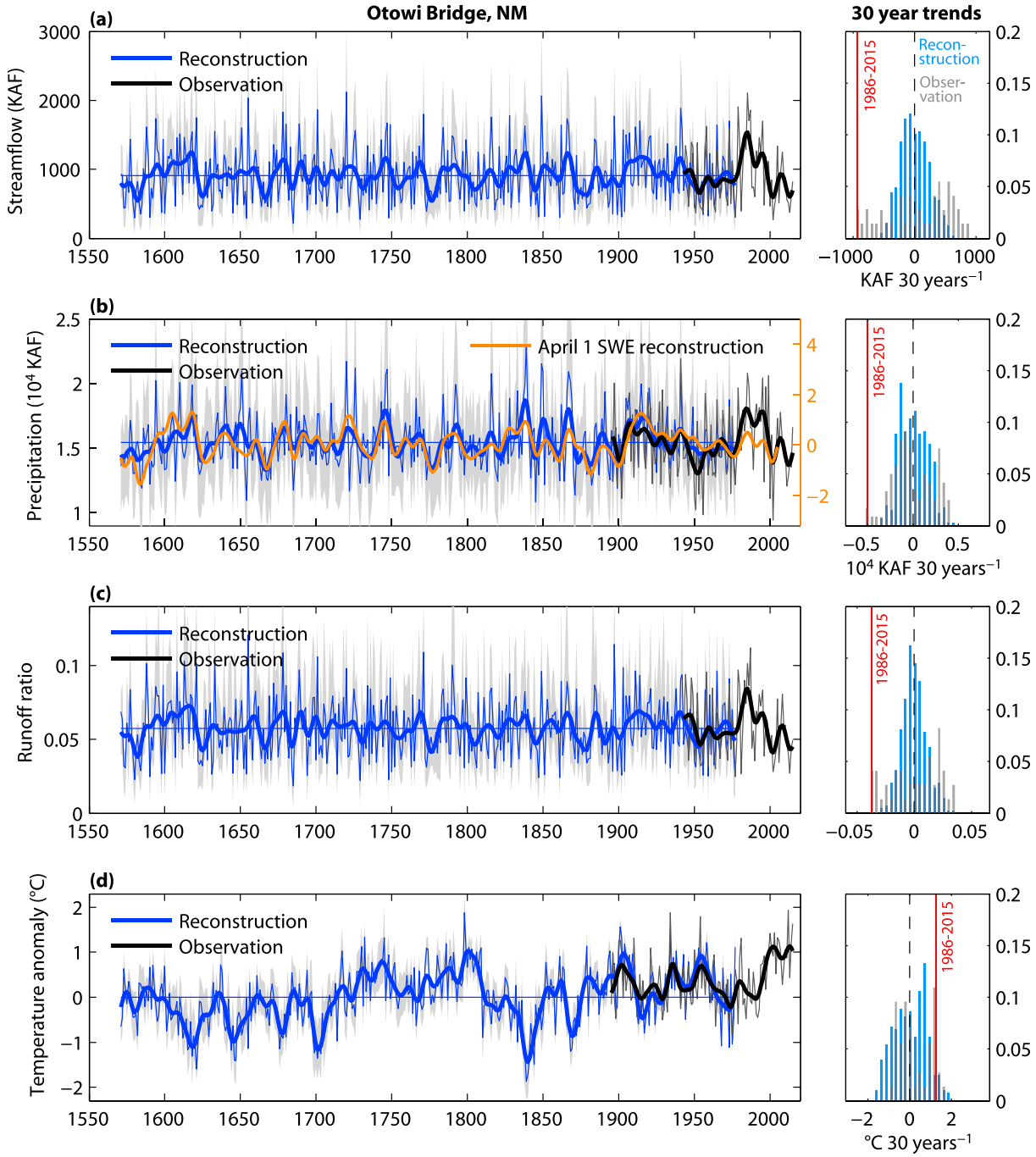

Figure 1. (left column) Time series of reconstructed (blue) and observed (black) (a) streamflow at Otowi Bridge in 1000 acre feet (KAF), (b) precipitation upstream of Otowi Bridge and normalized snow water equivalent (SWE; orange), (c) runoff ratio for Otowi Bridge, and (d) average surface air temperature upstream of Otowi Bridge. The thin lines are water year totals, except temperature, which are annual means, and SWE, which is 1 April. The thick lines are smoothed with a 10 year Fourier low-pass filter. The blue horizontal lines give the reconstruction mean 1571–1977. The thin gray shading indicates 5–95% reconstruction uncertainty. (right column) Normalized histograms of all 30 year trends of the water year/annual mean data. The red vertical line indicates the most recent 30 year trend 1986–2015. See section 2 for data sources and details.

2.2. Paleoclimate Reconstructions

We use existing tree ring-based reconstructions of water year (October–September) streamflow at the Otowi Bridge gauge, as well as water year precipitation and annual mean temperature over the associated drainage basin, covering a common period (1571–1977). The streamflow reconstruction uses moisture-sensitive tree

ring species, which reflect a combination of winter precipitation and summer evapotranspiration and thus capture key features of streamflow variability [*Woodhouse et al.*, 2012]. It was calibrated against naturalized flows in the 20th century and covers the period 1450–2012 C.E. (updated version; http://www.treeflow.info/content/rio-grande-owoti-new-mexico-update).

The precipitation reconstruction is a modified version of the 0.5° × 0.5° western U.S. precipitation reconstruction by *Diaz and Wahl* [2015], covering the period 1571–1977. The precipitation reconstruction relies on tree ring-based streamflow reconstructions, but, crucially for the study here, the streamflow reconstruction from Otowi Bridge has been excluded in the construction of this modified version. Thus, the streamflow and precipitation reconstructions used here are largely independent, with very few shared original chronologies (Table S1 and section S1 in the supporting information). To estimate precipitation in the Rio Grande basin upstream of Otowi Bridge, we spatially averaged the reconstructed precipitation over the aforementioned Otowi drainage region and multiplied it by the drainage area to obtain units of volume.

For annual mean temperature we extract a 5° × 5° grid cell centered at 37.5°N, 107.5°W (which corresponds roughly to the Rio Grande headwaters) from the reconstruction by *Wahl and Smerdon* [2012]. The coarse spatial resolution of this reconstruction does not weaken the analysis here because the length scale of high spatial correlation ($r > 0.8$) of the URG annual mean temperature encompasses the size of the selected grid cell in observations (Figure S1 in the supporting information). While the choice of annual mean is motivated by the available reconstruction data, we note that the annual mean and the more critical melt season (March–August) mean temperature in the URG basin are highly correlated ($r = 0.74$ in observations 1895–2015). For the determination of reconstruction uncertainties, see section S3.

2.3. Model Simulation

We use a 1800 year long preindustrial control simulation (piControl) from the Community Earth System Model (CESM), which is described in detail by *Kay et al.* [2015]. CESM is a fully coupled Earth System Model with components of atmosphere, ocean, sea ice, and land surface [*Hurrell et al.*, 2013]. In the configuration here, all components are run at ~1° × 1° horizontal resolution. The forcing represents perpetual 1850 C.E. conditions for atmospheric composition, orbital parameters, and land cover.

We extract streamflow from this simulation by extracting the routed runoff at the Otowi Bridge location from the 0.5° × 0.5° River Transport Model embedded in CESM. We recognize that the CESM runoff and routing schemes are coarse and contain climatological biases at the watershed scale, but we expect that they will sufficiently discriminate high and low flows driven by large-scale climate variations to be useful in the context of this study. CESM precipitation and surface air temperature are then extracted by mapping the Otowi Bridge drainage area onto the CESM grid.

3. Results

3.1. Hydroclimate Over the Past Four Centuries

At Otowi Bridge, streamflow has varied on interannual to decadal time scales, with pronounced periods of low flow as identified and discussed in *Woodhouse et al.* [2012]. Figures 1a and 1b show the reconstructed and observed time series of WY precipitation and streamflow for Otowi Bridge, Figure 1c shows the runoff ratio resulting from dividing streamflow by precipitation, and Figure 1d shows annual mean temperature. Beyond the decadal time scale, however, no prolonged periods of high or low flow were recorded in the reconstruction, consistent with other Southwestern U.S. findings that multidecadal drought conditions were more prevalent in the first half of the last millennium [*Cook et al.*, 2004; *Meko et al.*, 2007; *Coats et al.*, 2016], although there is a 16th century megadrought that ended just before our reconstructions begin [*Stahle et al.*, 2000]. Comparing the last four centuries of reconstructed streamflow to the recent decades of measured streamflow at Otowi Bridge clearly indicates that the observed annual high values of the 1980s and the low value of 2002 are exceptional, but not unprecedented. The highest value in the observations is 2074 KAF (1000 acre feet; in 1985) and the lowest value is 235 KAF (in 2002), whereas the highest reconstructed value is 2123 KAF (in 1720) and the lowest value is 216 KAF (in 1685). Due to uncertainties in the reconstruction [*Woodhouse et al.*, 2006], which are likely larger than the margin between the observed and reconstructed highest and lowest flows, it is uncertain but conceivable that these recent extrema are the highest and lowest flows in more than 400 years.

The 10 year smoothed time series (thick line in Figure 1a) clearly shows the 1980s to be the decade of highest flow over the whole time period, while the early 2000s tie within uncertainties with the 1580s and 1770s for the decade of lowest flow. Most importantly, the short sequencing of the exceptionally high- and low-flow decades within the last 30 years results in this period showing the strongest 30 year streamflow trends of the entire period of 1571–2015 (histogram in Figure 1a, at 99.1% probability; see section S4).

Precipitation is strongly correlated with streamflow (r = 0.75 in reconstructions 1571–1942, r = 0.89 in reconstructions 1943–1977, r = 0.77 in observations 1943–1977, and r = 0.79 in observations 1943–2015) and largely drove the extreme streamflow periods in both reconstructions and observations (Figure 1b). Precipitation is also strongly correlated (r = 0.73, 1571–1977) with a reconstruction of April snow water equivalent in the Rio Grande headwaters [*Pederson et al.*, 2011], suggesting that winter–spring precipitation can explain at least 50% of water year precipitation variability. Similar to streamflow, the 1980s stand out as an exceptional decade with precipitation values almost consistently above the long-term average derived from the reconstruction. Consequently, this wet decade and the subsequent decline into the generally drier 2000s also produced the strongest 30 year precipitation trend of the entire period (histogram in Figure 1b, at 97.9% probability). Interestingly, the 1990s were exceptionally wet as well but had lesser impact on the streamflow record than the 1980s (compare Figures 1a and 1b), leaving room for additional explanatory factors, as discussed later.

Due to the strong influence of precipitation on streamflow and runoff ratio in these arid regions [*Vano et al.*, 2012], the reconstructed time series of runoff ratio features many of the same high- and low-value periods as the precipitation reconstruction (Figure 1c). Again, the 1980s show exceptionally high runoff ratios and the decline into the early 2000s also marks the strongest 30 year trend in the entire period (histogram in Figure 1c, at 97.8% probability). However, there are a few periods, including the 1990s and the mid-19th century, in which the relationship between precipitation and runoff ratio appears to be weaker.

Compared to precipitation and streamflow, reconstructed temperature in the URG shows distinct multidecadal (relatively lower frequency) variations (Figure 1d). A roughly century-long cold period between 1600 and 1700 was followed by a similarly long period of above-long-term mean temperatures, followed by a sharp decrease and then gradual rise of temperature until present day. The highest reconstructed temperatures occurred in the late 18th century and rival the observed high values of the 20th and 21st centuries, although the past 15 years are clearly the warmest period of such length over the last 440+ years [cf. *Wahl and Smerdon*, 2012]. Unlike reconstructed streamflow, precipitation, and runoff ratio, observed 30 year temperature trends fall well within the distribution of the reconstruction.

3.2. Role of Temperature

While precipitation is the main driver of interannual streamflow variations in the URG, temperature also influences streamflow and hence runoff ratio. To investigate the role of temperature in interannual variations of runoff ratio, we plot runoff ratio (in percentile units) as a function of precipitation and temperature anomalies (Figure 2; all time series are relative to their median due to the non-Gaussian distribution of precipitation and runoff ratio, see Figure S2a). First, the figure illustrates the weak but statistically significant negative correlation between temperature and precipitation (r = −0.28 in reconstructions 1571–1942, r = −0.39 in reconstructions 1943–1977, r = −0.37 in observations 1943–1977, and r = −0.30 in observations 1943–2015) that is typical for this region [*Trenberth and Shea*, 2005] (correlation coefficients between −0.30 and −0.50 based on reanalysis data). Second, the stratification of high and low runoff ratio years according to associated precipitation anomalies clearly shows that positive precipitation anomalies are an important prerequisite for high runoff ratios with 76% of the years of high (>70th percentile) and 88% of the very high (>90th percentile) runoff ratios coinciding with positive precipitation anomalies in reconstructions (upper two quadrants in Figure 2a). In turn, 81% of the low (<30th percentile) and 95% of the very low (<10th percentile) runoff ratio years coincide with negative precipitation anomalies. Third, and most importantly for this study, a further stratification according to temperature shows that when precipitation is below the median, the low and very low runoff ratios are 1.7 and 2.5 times as likely to occur, respectively, in warm years (51% and 68%; bottom right quadrant in Figure 2a) than in cold years (30% and 27%; bottom left quadrant in Figure 2a). Also, there exists a significant correlation between runoff ratio and temperature that is almost entirely driven by the relationship of the two variables in dry years, with no significant correlation in wet years (Figures S2b–S2d).

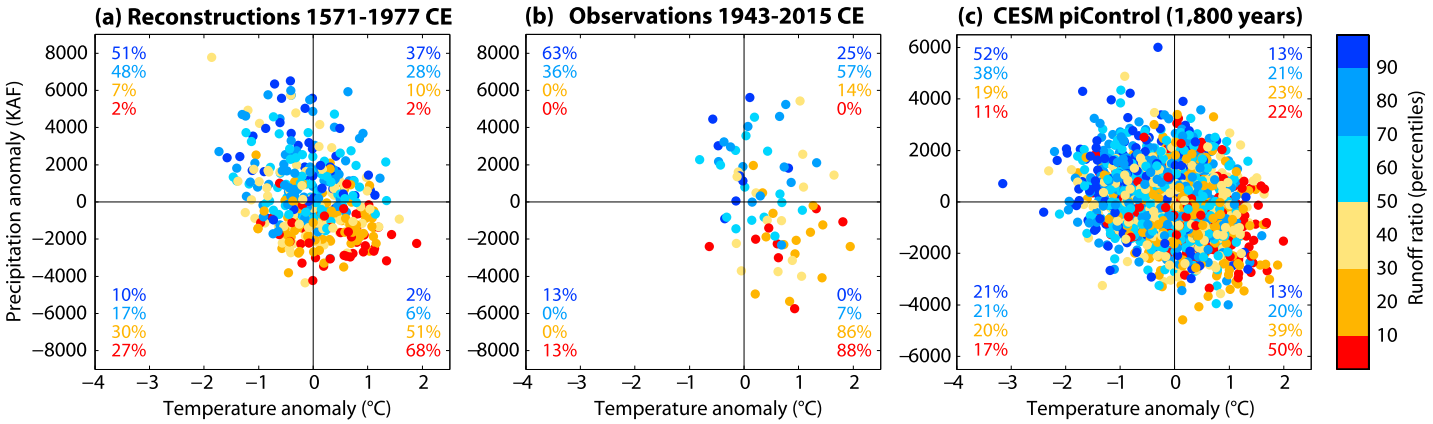

Figure 2. Runoff ratio at Otowi Bridge (colors) as a function of water year precipitation and annual mean temperature from (a) reconstructions, (b) observations, and (c) CESM control simulation (1800 years total). Time series are relative to their median, in the case of observations, relative to the median of the reconstructions. The colored numbers give the percentage of very low (<10th percentile), low (<30th), high (>70th), and very high (>90th) runoff ratio years that fall within a given quadrant of precipitation and temperature anomalies.

Repeating the analysis with reconstructions of summer and annual maximum monthly temperature does not alter these conclusions (section S5 and Figure S3).

The relationships found in the reconstructions are also clearly visible in the shorter (73 years) observational record (Figure 2b), which exhibits strong warming during the recent decades. In fact, 86% and 88% of all low and very low runoff ratio years, respectively, were dry and warm, while 0% and 13% of the low and very low runoff ratio years, respectively, were dry and cold. Notwithstanding the uncertainties due the small observational sample, the recent warm decades appear to have been an important factor in very low runoff ratio years.

Turning to the CESM simulation, we find that the model generally reproduces the sensitivities of runoff ratio that are found in the reconstructions and observations (Figure 2c): 59% of high runoff ratio years and 65% of very high runoff ratio years occur in wet years (above-median precipitation; top two quadrants in Figure 2c). In turn, 59% of low and 67% of very low runoff ratio years occur in dry years (below-median precipitation; bottom two quadrants in Figure 2c). Further, the apparent importance of high temperatures for the occurrence of very low runoff ratio years is found in CESM as well: 50% of the very low runoff ratio years occur in a dry and warm year, while only 17% occur in a dry and cold year, making it approximately 3 times as likely to have a very low runoff ratio year if temperatures are above normal rather than below normal (Figure 2c). Notable differences of the model output from the reconstructions and observations are the percentages of very high runoff ratio years when it is dry and cold, and the opposite very low runoff ratio years when it is wet and warm (Figure 2c, bottom-left and upper-right quadrants, respectively).

Due to the negative correlation between precipitation and temperature there exists a natural tendency for dry years to coincide with warm years. To account for this, we investigated the likelihood for very low/low/high/very high runoff ratios conditional on the background climate of the respective year and find the results reported above to be robust (section S6 and Figure S4).

3.3. Circulation Composites

To investigate the large-scale atmospheric circulation patterns potentially associated with certain cases of very high and low runoff ratios in the reconstruction, we search for analogous situations in CESM and create composite maps. Here we focus on the following four situations (using the very low/low/high/very high categories defined above): years with very high runoff ratio, high precipitation, and low temperature; years with very high runoff ratio, below-median precipitation, and below-median temperature; years with very low runoff ratio, below-median precipitation, and below-median temperature; and years with very low runoff ratio, low precipitation, and high temperature.

To construct the composites, we extract sea level pressure (SLP), precipitation, and temperature during the years that fulfill the above criteria from the CESM simulation and average them (Figure 3). Naturally, not all

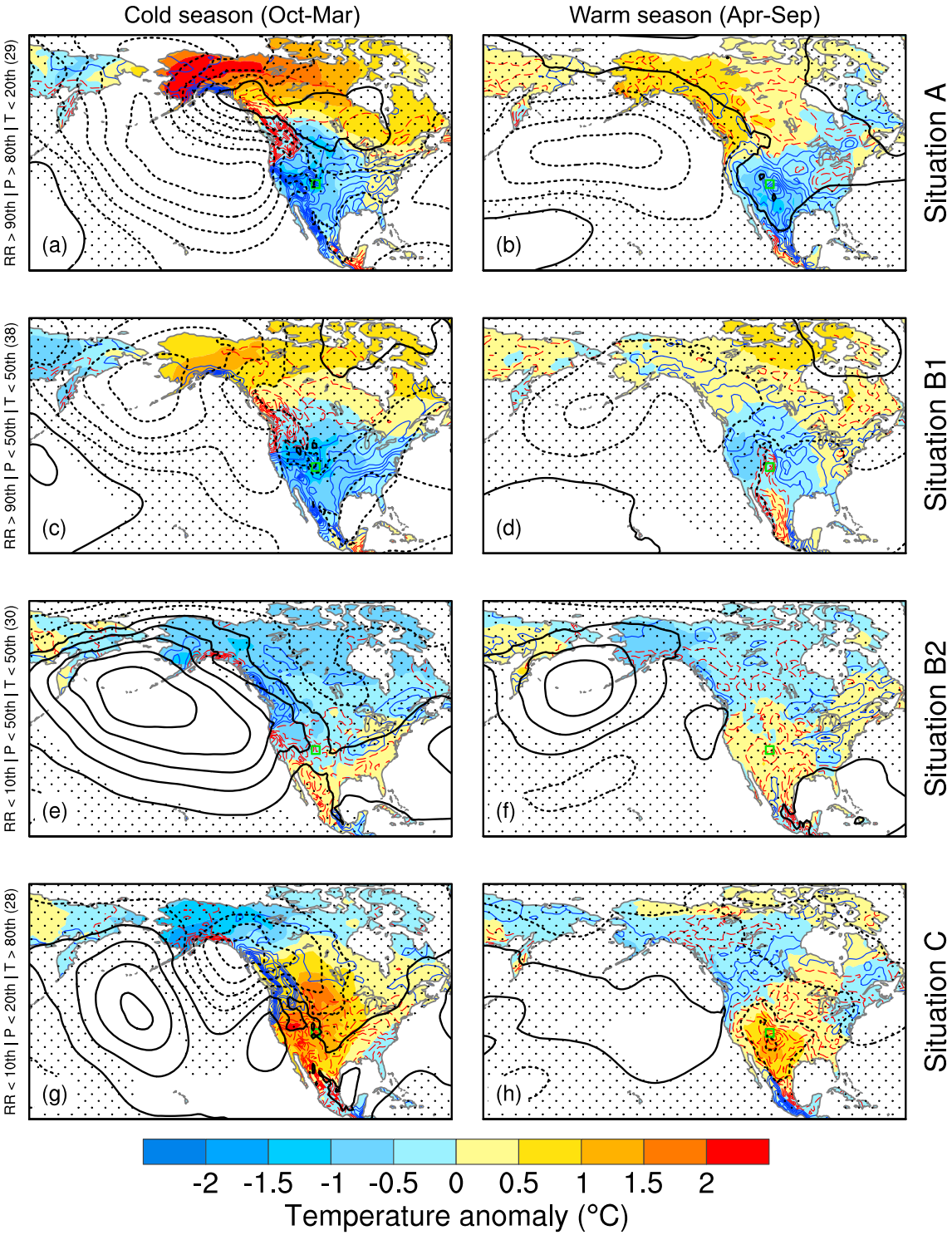

Figure 3. Composite situations from CESM control simulation of temperature (shading), precipitation (blue and red contours; increment of 0.1 mm/d, starting at ±0.05 mm/d), and sea level pressure (black contours; increment of 0.5 hPa, starting at ±0.25 hPa) anomalies for years with (a and b) very high runoff ratio (RR) while precipitation (P) is high and temperature (T) is low, (c and d) very high RR while both P and T are below median, (e and f) very low RR while both P and T are below median, and (g and h) very low RR while P is low and T is high. (left column) Cold season (October–March) means. (right column) Warm season (April–September) means. Negative anomalies are given as dashed contours. Stippling (sea level pressure) indicates nonsignificant difference at 95% probability level. The number of years forming each composite situation is given in brackets. The area of the Upper Rio Grande basin is indicated by the green square.

four situations occur with equal frequency in the 1800 model years analyzed; all four composites combined cover 9.3% of the 1800 total model years.

Situation A features a deep Aleutian Low over the North Pacific in both the cold (October–March) and warm (April–September) seasons, leading to a strong north-south temperature gradient across North America and high precipitation totals over much of the contiguous U.S. (hereafter "U.S."; Figures 3a and 3b). Both cold and warm season responses are robust over much of North America and the North Pacific (no stippling in Figure 3). Situation A in the cold season is reminiscent of the canonical El Niño response over the North Pacific-North America region. Indeed, 57% of all situations A coincide with winters (December–February) in which the Nino3.4 index (sea surface temperatures averaged over 170–120°W, −5 to 5°N) exceeds 1 standard deviation.

Situation B1, in which very high runoff ratios occur with below-median temperatures but in conjunction with below-median precipitation, shows a sharp contrast between cold and warm seasons in terms of circulation and precipitation (Figures 3c and 3d). The cold season features a wave train across the Pacific and North America, somewhat resembling the surface signature of the Pacific North American pattern. A deep Aleutian Low channels cold air from the Bering Sea to the U.S., while northern Canada receives positive temperature anomalies due to the southerly flow on the east side of the Aleutian Low (Figure 3c). Together with another low-pressure anomaly over the U.S. East Coast, these two SLP anomalies cause substantial positive precipitation anomalies across large parts of the U.S. In the warm season, the low-pressure anomaly over the Northeast Pacific is weaker and the SLP anomaly on the U.S. East Coast moves further inland (Figure 3d). The resulting flow across the central U.S. is predominantly northerly, causing dry and cold conditions and counteracting the moisture influx into the Southwestern U.S. that is typical for the North American summer monsoon. The contrasting precipitation totals from the cold and warm season result in a net negative water year precipitation anomaly, but due to the high accumulation in the cold season and the relatively cold warm season, runoff ratios remain very high.

Situation B2, in turn, during which very low runoff ratios occur during years of below-median precipitation and temperature, features a positive SLP anomaly over much of the northeastern Pacific in the cold season, diverting incoming storms from the Pacific to Canada and steering cold Arctic air across most of North America (Figure 3e). In the warm season, the positive SLP anomaly over the North Pacific is weaker and no clear circulation patterns are established over the U.S. (Figure 3f), although temperatures are slightly elevated and precipitation is slightly reduced over much of the western U.S. As a net result, this situation is mainly dominated by the cold season precipitation deficit, which, together with slightly above-average temperatures during the warm season, appears to be sufficient to drive very low runoff ratios.

Finally, situation C, during which some of the lowest runoff ratios of all CESM years occur, is in many ways the reversal of situation A, with high temperatures and low precipitation over most of the U.S. in both seasons (Figures 3g and 3h). The key features of the cold season composite are negative SLP anomalies over the Gulf of Alaska and a blocking high over the U.S. West Coast, steering storms into the northern half of the U.S. West Coast, while leaving the southern half of the coast and the central U.S. dry (Figure 3g). While resembling La Niña, only 38% of the winters in this composite show a Nino3.4 index <-1 standard deviation. In the warm season, the blocking high over the Pacific persists and a thermal low sets in over the central U.S., creating very warm and dry conditions and further decreasing streamflow relative to the precipitation decrease, thus causing anomalously low runoff ratios (Figure 3h).

All of these situations resemble viable climatological circulation patterns and can arise from unforced climate variability, as demonstrated by the use of a control simulation, which were found to contain substantial multidecadal variability of large-scale circulation patterns [*Deser et al.*, 2012a]. Our results therefore suggest that decadal variations in the frequency of these circulation patterns (for example, associated with the relative frequency of El Niño and La Niña events in recent decades) [*Meehl et al.*, 2009] might not, or only to a small degree, be associated with externally forced climate change, e.g., from increasing greenhouse gas concentrations. Due to the short observational record and the small signal-to-noise ratio of forced sea level pressure trends in simulations [*Deser et al.*, 2012b], detection and attribution of anthropogenically forced changes in observed circulation patterns and hydroclimate over the American Southwest remain an active area of research [*Prein et al.*, 2016].

4. Summary and Conclusions

In summary, paleoclimate reconstructions suggest that both the high and low annual runoff ratios of the most recent decades in the URG were extreme in context of the last 440 years. As a consequence, the 30 year declining trend in runoff ratio from the mid-1980s to present day appears to be unprecedented and is problematic for current statistical seasonal streamflow forecasting approaches that assume hydroclimatic stationarity. Although decadal-scale trends in runoff ratio are driven primarily by precipitation variations, the paleoclimate record also reveals an important role for temperature in creating some of the lowest runoff ratio years in the last four centuries. Supported by a long climate model simulation, we estimate that in years with below-median precipitation, very low (<10th percentile) runoff ratios are 2.5–3 times more likely if temperatures are warmer than normal (above-median).

If recent warming trends continue, our findings suggest a further decline in runoff ratios in the URG and other Southwestern U.S. basins. Nevertheless, the paleoclimate record and associated circulation composites indicate that low and high runoff ratios of almost equal magnitude as observed in recent decades are possible in the absence of any significant greenhouse gas forcing trend. In this light, careful detection and attribution is warranted when diagnosing underlying causes of recent hydroclimate trends in the Southwestern U.S.

Acknowledgments

We thank Andrew Newman, Keith Musselmann, Kevin Sampson, and Nabil Shafike for discussion or technical support, as well as two anonymous reviewers for their very constructive feedback. Part of this work was inspired by a workshop held at the Lamont-Doherty Earth Observatory of Columbia University on 1–3 June 2016, titled "Comparing data and model estimates of hydroclimate variability and change over the Common Era." We acknowledge the efforts of all those who contributed to producing the CESM LE and the paleoclimate reconstructions. The CESM simulation is available on the Earth System Grid (www.earthsystemgrid.org), the reconstructions will be made available at NOAA Paleoclimatology (www.ncdc.noaa.gov/data-access/paleoclimatology-data/datasets), the Otowi Index Supply is available from the corresponding author. The National Center for Atmospheric Research is sponsored by the National Science Foundation. F.L. is supported by a Postdoc Applying Climate Expertise (PACE) fellowship cosponsored by NOAA and the Bureau of Reclamation. A.W.W. is supported by Reclamation under Cooperative Agreement #R11AC80816 and by the U.S. Army Corps of Engineers (USACE) Climate Preparedness and Resilience Program. F.L. designed the study, conducted the analysis, and led the writing; E.R.W. created all new reconstructions; E.R.W. and A.W.W. helped design the study; and all authors contributed to the writing.

References

Alley, W. M., R. W. Healy, J. W. LaBaugh, and T. E. Reilly (2002), Flow and storage in groundwater systems, *Science*, *296*, 1985–1990, doi:10.1126/science.1067123.

Bureau of Reclamation (2016), *Climate Change Adaptation Strategy*, 33 pp., Bureau of Reclamation, Washington, D. C. [Available at https://www.usbr.gov/climate/docs/2016ClimateStrategy.pdf.]

Coats, S., J. E. Smerdon, R. Seager, D. Griffin, and B. I. Cook (2015), Winter-to-summer precipitation phasing in southwestern North America: A multicentury perspective from paleoclimatic model-data comparisons, *J. Geophys. Res. Atmos.*, *120*, 8052–8064, doi:10.1002/2015JD023085.

Coats, S., J. E. Smerdon, K. B. Karnauskas, and R. Seager (2016), The improbable but unexceptional occurrence of megadrought clustering in the American West during the Medieval climate anomaly, *Environ. Res. Lett.*, *11*, 74025, doi:10.1088/1748-9326/11/7/074025.

Cook, E. R., C. A. Woodhouse, C. M. Eakin, D. M. Meko, and D. W. Stahle (2004), Long-term aridity changes in the western United States, *Science*, *306*, 1015–1018, doi:10.1126/science.1102586.

Dahm, C. N., R. J. Edwards, and F. P. Gelwick (2005), Gulf Coast rivers of the Southwestern United States, *Rivers North Am.*, 180–228.

Daly, C., M. Halbleib, J. I. Smith, W. P. Gibson, M. K. Doggett, G. H. Taylor, J. Curtis, and P. P. Pasteris (2008), Physiographically sensitive mapping of climatological temperature and precipitation across the conterminous United States, *Int. J. Climatol.*, *28*, 2031–2064, doi:10.1002/joc.1688.

Deser, C., et al. (2012a), ENSO and pacific decadal variability in the community climate system model version 4, *J. Clim.*, *25*, 2622–2651, doi:10.1175/JCLI-D-11-00301.1.

Deser, C., A. Phillips, V. Bourdette, and H. Teng (2012b), Uncertainty in climate change projections: The role of internal variability, *Clim. Dyn.*, *38*, 527–546, doi:10.1007/s00382-010-0977-x.

Dettinger, M. D., and D. R. Cayan (1995), Large-scale atmospheric forcing of recent trends towards early snowmelt runoff in California, *J. Clim.*, *8*, 606–623, doi:10.1175/1520-0442(1995)008<0606:LSAFOR>2.0.CO;2.

Diaz, H. F., and E. R. Wahl (2015), Recent California water year precipitation deficits: A 440-year perspective, *J. Clim.*, *28*, 4637–4652, doi:10.1175/JCLI-D-14-00774.1.

Franz, K. J., H. C. Hartmann, S. Sorooshian, and R. Bales (2003), Verification of National Weather Service Ensemble Streamflow Predictions for water supply forecasting in the Colorado River basin, *J. Hydrometeorol.*, *4*, 1105–1118, doi:10.1175/1525-7541(2003)004<1105:VONWSE>2.0.CO;2.

Griffin, D., et al. (2013), North American monsoon precipitation reconstructed from tree-ring latewood, *Geophys. Res. Lett.*, *40*, 954–958, doi:10.1002/grl.50184.

Hamlet, A. F., P. W. Mote, M. P. Clark, and D. P. Lettenmaier (2005), Effects of temperature and precipitation variability on snowpack trends in the western United States, *J. Clim.*, *18*, 4545–4561, doi:10.1175/JCLI3538.1.

Hurrell, J. W., et al. (2013), The Community Earth System Model: A framework for collaborative research, *Bull. Am. Meteorol. Soc.*, *94*, 1339–1360, doi:10.1175/BAMS-D-12-00121.1.

Kay, J. E., et al. (2015), The Community Earth System Model (CESM) large ensemble project: A community resource for studying climate change in the presence of internal climate variability, *Bull. Am. Meteorol. Soc.*, *96*(8), 1333–1349, doi:10.1175/BAMS-D-13-00255.1.

Meehl, G. A., A. Hu, and B. D. Santer (2009), The mid-1970s climate shift in the pacific and the relative roles of forced versus inherent decadal variability, *J. Clim.*, *22*, 780–792, doi:10.1175/2008JCLI2552.1.

Meko, D. M., C. A. Woodhouse, C. A. Baisan, T. Knight, J. J. Lucas, M. K. Hughes, and M. W. Salzer (2007), Medieval drought in the Upper Colorado River basin, *Geophys. Res. Lett.*, *34*, L10705, doi:10.1029/2007GL029988.

Pagano, T., D. Garen, and S. Sorooshian (2004), Evaluation of official western U.S. seasonal water supply outlooks, 1922–2002, *J. Hydrometeorol.*, *5*, 896–909, doi:10.1175/1525-7541(2004)005<0896:EOOWUS>2.0.CO;2.

Pagano, T., A. Wood, K. Werner, and R. Tama-Sweet (2014), Western U.S. water supply forecasting: A tradition evolves, *Eos Trans. AGU*, *95*, 28–29, doi:10.1002/2014EO030007.

Painter, T. H., J. S. Deems, J. Belnap, A. F. Hamlet, C. C. Landry, and B. Udall (2010), Response of Colorado River runoff to dust radiative forcing in snow, *Proc. Natl. Acad. Sci. U.S.A.*, *107*, 17,125–17,130, doi:10.1073/pnas.0913139107.

Pederson, G. T., et al. (2011), The unusual nature of recent snowpack declines in the North American cordillera, *Science*, *333*, 332–335, doi:10.1126/science.1201570.

Prein, A. F., G. J. Holland, R. M. Rasmussen, M. P. Clark, and M. R. Tye (2016), Running dry: The U.S. Southwest's drift into a drier climate state, *Geophys. Res. Lett.*, *43*, 1272–1279, doi:10.1002/2015GL066727.

Rosenberg, E. A., A. W. Wood, and A. C. Steinemann (2011), Statistical applications of physically based hydrologic models to seasonal streamflow forecasts, *Water Resour. Res.*, *47*, W00H14, doi:10.1029/2010WR010101.

Serreze, M. C., M. P. Clark, R. L. Armstrong, D. A. McGinnis, and R. S. Pulwarty (1999), Characteristics of the western United States snowpack from snowpack telemetry (SNOTEL) data, *Water Resour. Res.*, *35*, 2145–2160, doi:10.1029/1999WR900090.

Stahle, D. W., E. R. Cook, M. K. Cleaveland, M. D. Therrell, D. M. Meko, H. D. Grissino-Mayer, E. Watson, and B. H. Luckman (2000), Tree-ring data document 16th century megadrought over North America, *Eos Trans. AGU*, *81*, 121–125, doi:10.1029/00EO00076.

Trenberth, K. E., and D. J. Shea (2005), Relationships between precipitation and surface temperature, *Geophys. Res. Lett.*, *32*, L14703, doi:10.1029/2005GL022760.

Udall, B., and J. Overpeck (2017), The 21st century Colorado River hot drought and implications for the future, *Water Resour. Res.*, doi:10.1002/2016WR019638.

Vano, J. A., T. Das, and D. P. Lettenmaier, 2012: Hydrologic sensitivities of Colorado River runoff to changes in precipitation and temperature. *J. Hydrometeorol.*, *13*, 932–949, doi:10.1175/JHM-D-11-069.1.

Wahl, E. R., and J. E. Smerdon, 2012: Comparative performance of paleoclimate field and index reconstructions derived from climate proxies and noise-only predictors. *Geophys. Res. Lett.*, *39*, L06703, doi:10.1029/2012GL051086.

Woodhouse, C. A., S. T. Gray, and D. M. Meko (2006), Updated streamflow reconstructions for the Upper Colorado River basin, *Water Resour. Res.*, 42, W05415, doi:10.1029/2005WR004455.

Woodhouse, C. A., D. W. Stahle, and J. V. Diaz (2012), Rio Grande and Rio Conchos water supply variability over the past 500 years, *Clim. Res.*, *51*, 147–158, doi:10.3354/Cr01059.

Woodhouse, C. A., D. M. Meko, D. Griffin, and C. L. Castro (2013), Tree rings and multiseason drought variability in the Lower Rio Grande basin, USA, *Water Resour. Res.*, *49*, 844–850, doi:10.1002/wrcr.20098.

Woodhouse, C. A., G. T. Pederson, K. Morino, S. A. McAfee, and G. J. McCabe (2016), Increasing influence of air temperature on Upper Colorado River streamflow, *Geophys. Res. Lett.*, *43*, 2174–2181, doi:10.1002/2015GL067613.